OBSERVATIONS AND MITIGATION OF RFI IN ALOS PALSAR SAR DATA; IMPLICATIONS FOR THE DESDYNI MISSION

Paul A. Rosen, Scott Hensley, and Charles Le

Jet Propulsion Laboratory, California Institute of Technology
4800 Oak Grove Drive, Pasadena, CA, 91109, USA
phone: +1 818 354 0023, fax: +1 818 393 5285, email: Paul.A.Rosen@jpl.nasa.gov
web: www.jpl.nasa.gov

Keywords: SAR, InSAR, RFI

ABSTRACT

Initial examination of ALOS PALSAR synthetic aperture radar (SAR) data has indicated significant radio frequency interference (RFI) in several geographic locations around the world. RFI causes significant reduction in image contrast, introduces periodic and quasi-periodic image artifacts, and introduces significant phase noise in repeat pass interferometric data reduction. The US National Research Council Decadal Survey of Earth Science has recommended DESDynI, a Deformation, Ecosystems, and Dynamics of Ice satellite mission comprising an L-band polarimetric radar configured for repeat pass interferometry. There is considerable interest internationally in other future L-band and lower frequency systems as well. Therefore the issues of prevalence and possibilities of mitigation of RFI in these crowded frequency bands is of considerable interest. RFI is observed in ALOS PALSAR in California, USA, and in southern Egypt in data examined to date. Application of several techniques for removing it from the data prior to SAR image formation, ranging from straightforward spectral normalization to time-domain, multi-phase filtering techniques are considered. Considerable experience has been gained from the removal of RFI from P-band acquired by the GeoSAR system. These techniques applied to the PALSAR data are most successful when the bandwidth of any particular spectral component of the RFI is narrow. Performance impacts for SAR imagery and interferograms are considered in the context of DESDynI measurement requirements.

1. INTRODUCTION

The era of Earth Observing Systems missions for Earth Science at NASA is coming to an end, with all planned satellites in orbit acquiring data. NASA is currently planning its observing strategy for the next decade, and commissioned the National Research Council (NRC) to conduct a Decadal Survey of Earth Sciences[1]. The Decadal Survey was completed in January 2007. The NRC formulated a chronological plan for critical Earth Science missions to be flown over the next decade. The Survey recommended that NASA proceed with a number of missions immediately. One of these missions was called DESDynI (Deformation, Ecosystem Structure, and Dynamics of Ice), comprising both interferometric radar and multiple-beam lidar sensors to measure surface deformation for understanding natural hazards and climate and vegetation structure for understanding ecosystem health. The lidar needs to yield statistically-valid sampling of the Earth's vegetated surface over the life of the mission, and radar coverage needs to be at short (about 8 day) repeat intervals for resolution of rapid geophysical processes and for minimizing atmospheric delay variations in InSAR products. The radar should operate within the L-band portion of the spectrum, with large enough bandwidth to allow accurate ionospheric corrections. Horizontal spatial radar resolution should be about 20 m, the lidar spot size should be about 25 m, and vertical accuracies of the InSAR and lidar should be 1-2 mm and 2-10 cm, respectively. The major scientific objectives for DESDynI defined by the Decadal Survey are:

- Determine the likelihood of earthquakes, volcanic eruptions, and landslides
- Characterize the effects of changing climate and land use on species habitats and carbon budget.
- Predict the response of ice sheets to climate change and impact on sea level.
- Monitor the migration of fluids associated with hydrocarbon production and groundwater resources.

NASA hosted a workshop from July 17-19, 2007 in Orlando, Florida for the purpose of assessing the NRC Decadal Study recommendation that NASA implement the DESDynI Mission concept [2]. Among the recommendations that came out of the workshop was the call to study implementation options for the mission, including spacecraft and instrument trade studies.

One of the key issues with L-band radar that will factor into these trade studies is the quality of the data in the presence of radio frequency interference. RFI causes significant reduction in image contrast, introduces periodic and quasi-periodic image artifacts, and introduces significant phase noise in repeat pass interferometric data reduction, a key product of the DESDynI mission. Initial examination of ALOS PALSAR synthetic aperture radar (SAR) data [3] has indicated significant radio frequency interference (RFI) in several geographic locations around the world. In this paper, we describe some of these observations and their effects on image quality.

2. IMAGE OBSERVATIONS

The existence of RFI in airborne radar data is well-known, and much work has been done to attempt to mitigate it. Observations of spaceborne radar interference are more limited, and we therefore are surveying ALOS PALSAR L-band SAR data to look for RFI. Our initial test sites are in California and Egypt. RFI has been seen in SIR-C and Seasat L-band data in the past in California, and the Middle East is known to have significant ground-based radiating systems in these bands.

2.1 Raw Data Observations of RFI

Figure 1 shows a segment of a spectrogram from raw SAR data acquired in Egypt by ALOS PALSAR. Radar range frequency is the dimension across, and pulse number the dimension down. The spectrum is centered such that the center of the spectrum is at the left edge of the image. The characteristic shape of the range reference function, with the ringing at the outer edges of the passband, is clear. The bright structured banding across the spectrum that shows up intermittently and with variable bandwidth is RFI.

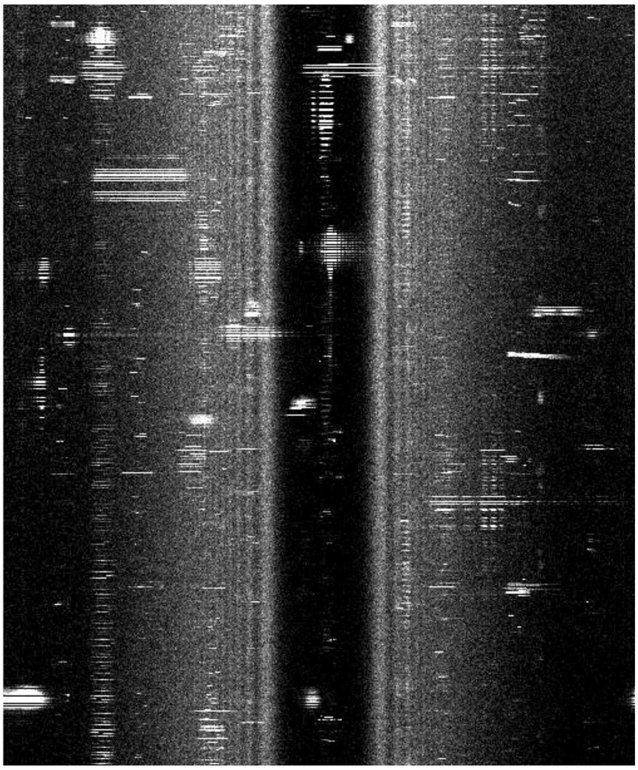

Figure 1 – Illustration of RFI in the ALOS PALSAR L-band raw data acquired over Egypt in 2007. Range frequency is across, with zero at the left and right edges, and the half the complex sampling frequency in the center. Time increases downward. The bandwidth of the data is approximately 28 MHz.

Figure 2 – Area of where data illustrated in Fig. 1 was acquired is from Nabta Playa (circled in red) in the south of Egypt, far from Egyptian urban centers.

This is a tremendously complicated RFI environment, with many broadband sources intermittently received. Many of the simpler mitigation schemes that rely on narrow-band and regular peaks in the spectrum will not be effective. Figure 2 shows the area of southern Egypt where the data were acquired. This area is centered on Nabta Playa, a site of significant archaeological interest, where interferometric studies of sand penetration would be of considerable value. ALOS PALSAR acquired only one image of the area in its first two years of operations, but further images of potential interferometric quality are scheduled for acquisition.

2.2 Processed Imagery

We processed the data whose spectrum is shown in Fig. 1 with no RFI removal. The resulting overall image is shown in Fig. 3. The region depicted is in southern Egypt, which is very arid, covered mostly in sand and alluvium. The features seen are likely to be representative of the rocky surface below the sand cover, as was observed by the Shuttle Imaging Radars in the 1980s and 1990s. A small portion of the image illustrating the RFI impact on a local scale is shown in Fig. 4. Though it is difficult to see the RFI at this spatial scale, there is evidence of RFI in the darker regions, showing up as banding artifacts, and an overall brightness patina limiting contrast in the image.

The detail in Fig. 4 shows the RFI more clearly. The RFI at this spatial scale is clearly visible as periodic wave-like brightness variations across the swath. Different textures can be seen on the left and right portions of the image. This magnitude of interference clearly limits the interpretability of

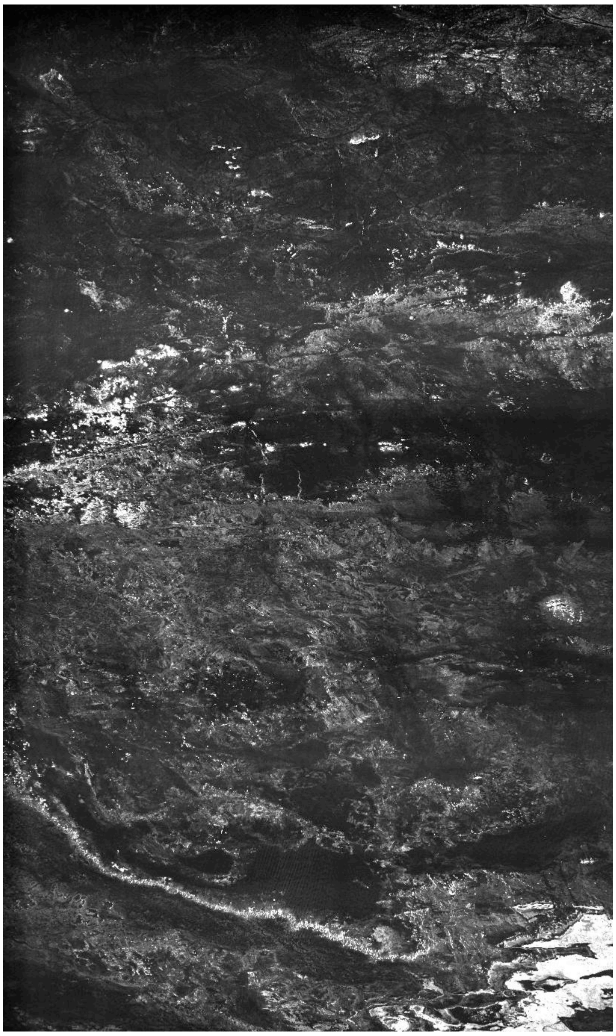

Figure 3 – Processed ALOS PALSAR L-band image. Data acquired over Egypt in 2007. Range dimension is across and along track dimension is down. The image is roughly 100 km x 200 km.

the data. Features such as those in Fig. 4 destroy the radiometric accuracy of the data, rendering interpretation of backscatter in terms of biomass, an important DESDynI objective, limited (note: there is no biomass in this example from Egypt). There is also risk that such features cannot be distinguished from true landforms with similar structure, such as sand dunes. In severe cases such as Fig. 4, the interpretation is relatively easy to determine, but not all cases are as clear.

3. INSAR OBSERVATIONS

Repeat-pass interferometric reduction [4] of ALOS PALSAR data has been performed for a handful of data. Because of the campaign strategy of the mission and the long repeat period, there is not an abundance of interferometric data yet at this point in the mission. Figure 5 shows a small portion of an interferogram produced over California exhibiting RFI. In both the image brightness (overlaid on the interferometric phase that is rendered in color) and the phase, there is clear evidence of RFI corruption of the signal. The undulations of the phase on the right edge of the

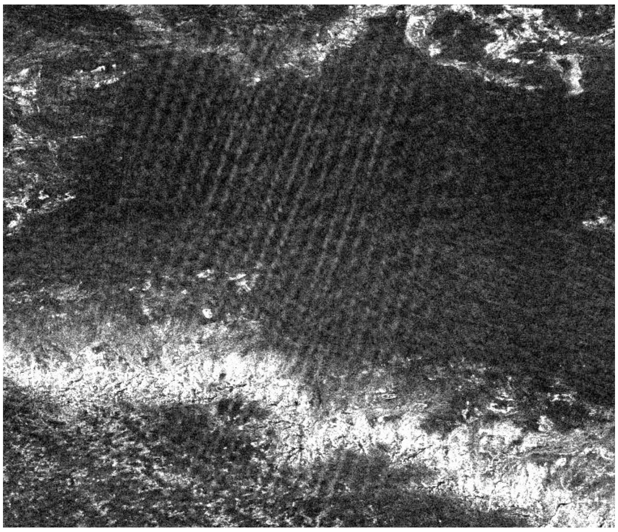

Figure 4 – Detail of processed ALOS PALSAR L-band image shown in Fig. 3. Range dimension is across and along track dimension is down. The image is roughly 7 km x 6 km.

image is a significant fraction of the L-band cycle (12 cm one-way delay), so represents a very large error in what would normally be interpreted as a deformation signal. Such errors are a considerable limitation to making accurate measurements of deformation in a mission like DESDynI, so it is important to understand their prevalence and possibility to mitigate them. Similar signals have been seen in other interferometric data acquired over southern California.

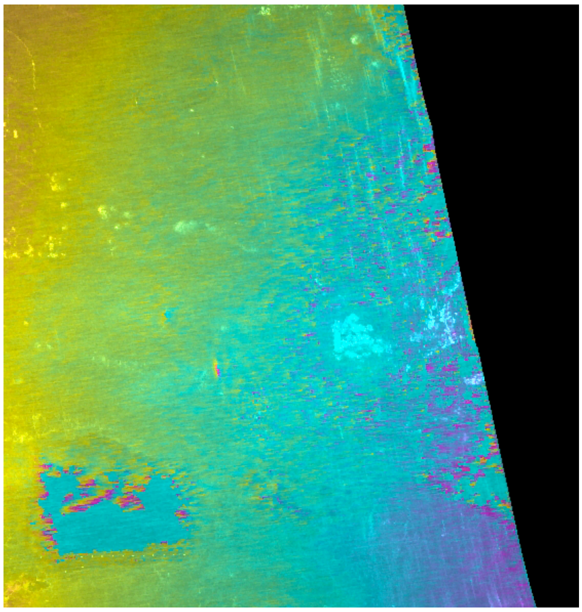

Figure 5 – Segment of processed ALOS PALSAR L-band geocoded interferogram, showing effects of RFI on the interferometric phase. Image size is approximately 20 km x 20 km.

Figure 6 shows another example of RFI in repeat pass interferometric data acquired over the big island of Hawaii. These data show a very limited signature in both spectral and temporal extent. The RFI is limited in time to just when the satellite is over Kilauea itself, which unfortunately in this case is where the deformation signal of interest occurs. The

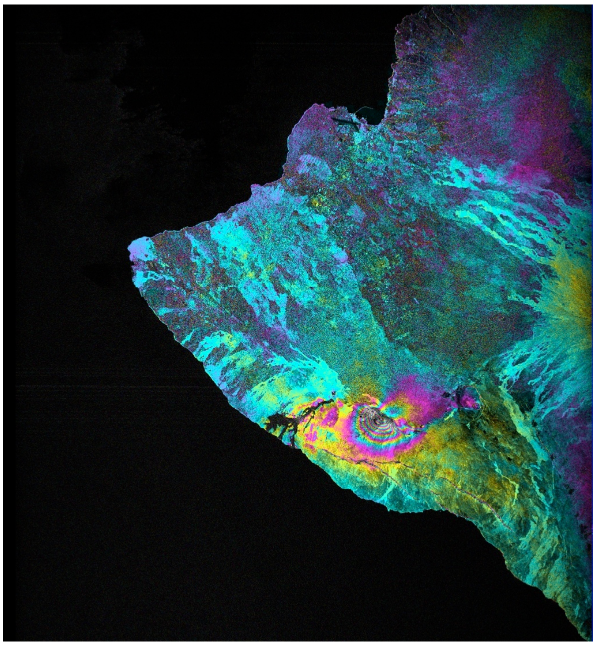

Figure 6 –ALOS PALSAR L-band interferogram over the big island of Hawaii. The topography has been removed showing only the deformation signal from a dike intrusion. RFI effects on the phase are undetectable at this scale as it is a small effect.

interferogram shown in Fig. 6 does not exhibit any obvious phase anomalies due to the small amount of RFI present. The effect of the RFI is most easily detected in the correlation measurements, as shown in Fig. 7. The correlation clearly has horizontal bands of lowered values in the vicinity of the caldera itself, extending over the surrounding region. Lowered correlation indicates an increase in measurement noise, hence bands of lowered deformation accuracy are introduced by the RFI in this case. Since the deformation signal is quite large in this case, the effects of this are negligible, however in cases where the deformation signal is more subtle, such decorrelation effects can be of greater significance, so mitigation can become more important.

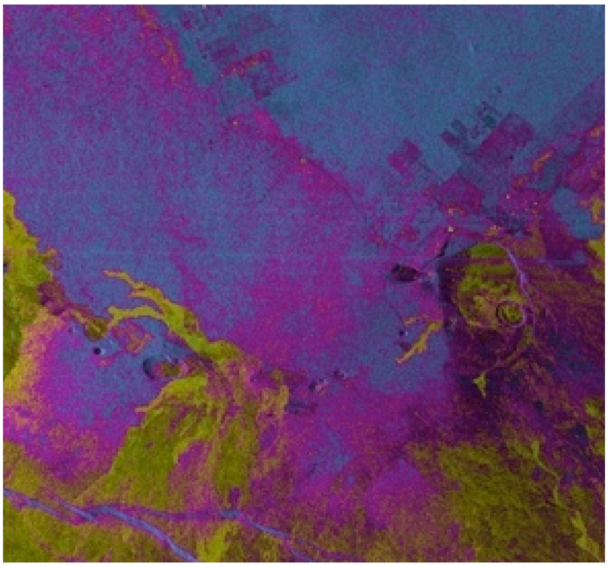

Figure 7 –Correlation detail showing bands of decorrelation running horizontally across the image. Yellow-green indicated very high correlation, seen on lava flows. Magenta is lower and blue is lowest correlation. Decreased correlation implies higher phase noise in the measurement.

4. MITIGATION

In order to obtain maximal quality imagery and interferometric products, it is desirable to remove the RFI signal prior to processing. If the RFI is very narrowband and fairly persistent, a simple notch filter suffices to adequately remove the RFI. However, in more complex RFI environments where the RFI is changing from pulse-to-pulse, varies with polarization, and exhibits complex spectral characteristics, simple notch filtering does not suffice due to the unacceptable loss of image resolution and image quality (e.g. SNR and ISLR). In order to maintain image equality, an RFI filter that coherently subtracts the RFI with a pulse-to-pulse adaptive filter is needed.

As part of the NASA/JPL GeoSAR program, we developed as a class of RFI removal algorithms based on the least-mean-square (LMS) adaptive filter algorithm. The software applies the least-mean-square (LMS) adaptive filter to suppress narrow-band radio-frequency interference (RFI) in wideband radars. We have implemented three versions of the LMS algorithms: the time-domain LMS (TDLMS), the frequency-domain LMS (FDLMS), and the filter-bank LMS (FBLMS) adaptive filters. The FBLMS method is used in practice since it is the most efficient of the filtering methods and has the best RFI removal properties. In addition to the basic LMS algorithm the software also employs several additional techniques, such as the median filter, spectral estimation, and the variable step-size algorithm, for the automatic determination of the LMS filter's parameters. Some of the advantages of the algorithm include:

1. Coherent subtraction of RFI contaminants from the received signal leads to phase preservation for aperture synthesis in SAR, polarization synthesis in radar polarimetry, and interferogram generation in InSAR. This is in contrast of the traditional approach of spectrum notching in the frequency domain.
2. There is no need to model the RFI environment as a sum of narrowband radiators, whose frequency, amplitude, and phase are estimated, for each RFI source. In contrast, the RFI environment as a whole is modeled as an autoregressive process, narrowband with respect to the radar bandwidth. Hence, most of the RFI signals, narrow and wideband, are estimated in one pass of the adaptive filter.
3. The software can be run in both manual and automatic modes. In the manual mode, the user determines the filter's parameters. In the automatic mode, the software implements a number of techniques (with strong theoretical bases, such as the median filter, the variable step-size algorithm, spectral estimation) to yield judicious choices for the filter's parameters. In the manual mode, the parameters are kept constant throughout the execution of the program. In the automatic mode, the parame-

ters are adaptively changed as a function of the inputs, resulting in better overall performance.

We have applied these RFI removal methods to improve the imagery acquired over Egypt. Though the signals seen in the Egypt ALOS data are not particularly narrow band, the performance of the algorithm is quite good, as shown in the following figures.

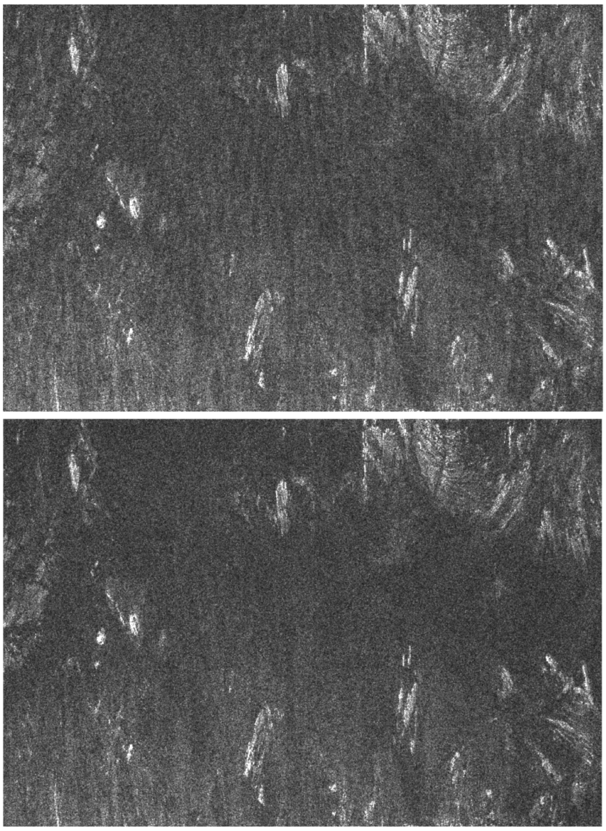

Figure 8 –Top image shows a portion of Fig. 3 with original RFI observed present in the data. The lower panel shows the same area with the NASA/JPL GeoSAR RFI removal algorithm applied. Note that the characteristic overlay of cross-hatched spurious signals have been removed, and the overall image contrast is greatly improved.

Figure 9 shows the result of applying the RFI removal algorithm to the entire image in summary form. Even in this challenging RFI environment, the spectrum becomes much cleaner after filtering. While some small RFI residual are evident in the filtered data of the top panel, it is not evident in the processed data in the bottom panel. This is because the matched filtering operation of image formation spreads the narrowband energy around the spectrum and contributes to overall multiplicative noise budget.

5. SUMMARY

Significant radio frequency interference signals have been seen in L-band ALOS PALSAR SAR data. The effects on image brightness and interferometric quality are apparent in

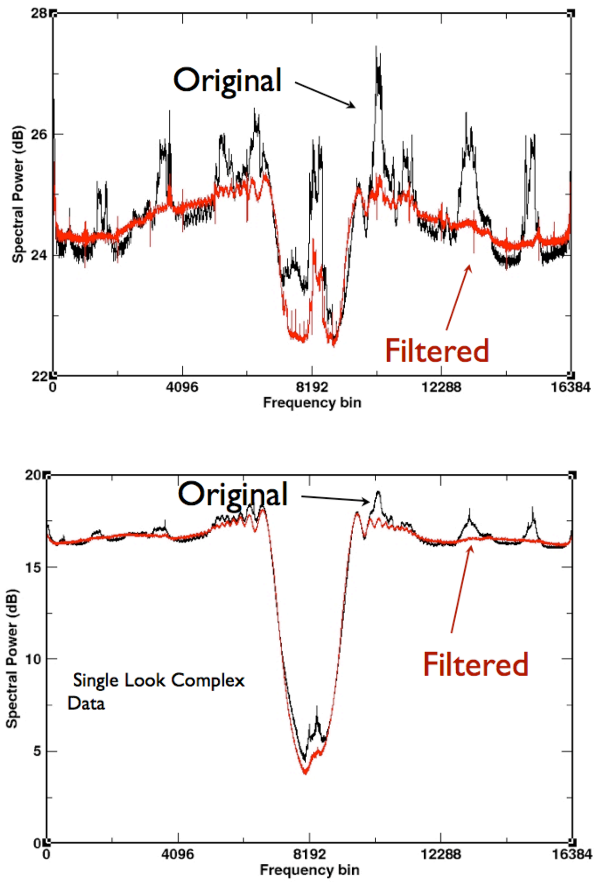

Figure 9 –Top panel shows accumulated spectra of the raw ALOS PALSAR data both before and after RFI removal filtering. The bottom panel shows accumulated spectra after image formation using unfiltered (black) and RFI-filtered (red) raw data.

some of the very first images we have processed from the satellite, indicating that RFI is likely to be a significant contributor to the overall error budget for an L-band sensor if the RFI is not mitigated. The spectrum of data acquired over Egypt is replete with broadband and intermittent RFI signatures. Less severe, but significant, RFI has been seen in interferograms of data acquired over California and Hawaii as well. Current evidence of the prevalence of the RFI is anecdotal and must be studied in more detail through a more comprehensive survey of data. Once the nature and global distribution of L-band RFI is known, mitigation techniques can be applied to attempt to remove it. RFI may well be the limiting factor in noise performance in a number of geographic areas. Experiments with RFI filtering techniques on ALOS PALSAR data have been quite successful for imagery, but more work is needed to assess interferometric performance after filtering. Based on these results on imagery, it appears highly likely that an increasingly complex RFI environment at L-band will be manageable for the DESDynI mission. However, computational complexity increases dramatically if all data must be cleaned prior to processing. Hence, developing methods for selective RFI removal may be required.

Acknowledgments This work was performed at the Jet Propulsion Laboratory, California Institute of Technology, under contract with the National Aeronautics and Space Administration. The authors would like to thank Eric Fielding and Bruce Chapman of JPL for providing an example of a processed interferogram exhibiting RFI, and Howard Zebker of Stanford University for data and helpful discussions.

REFERENCES

[1] Earth Science and Applications from Space:National Imperatives for the Next Decade and Beyond, The National Acadamies Press, 2007.

[2] DESDynI Workshop Report 2007 http://cce.nasa.gov/desdyni/

[3] http://www.eorc.jaxa.jp/ALOS/

[4] Rosen, P.A., S. Hensley, G. Peltzer and M. Simons, Updated Repeat Orbit Interferometry Package Released, EOS, Trans. of the Amer. Geophys. Un., v. 85, 2004, doi 10.1029/2004EO050004.

[5] Hensley, S.; Chapin, E.; Freedman, A.; Le, C.; Madsen, S.; Michel, T.; Rodriguez, E.; Siqueira, P.; Wheeler, K. (2001) First P-band results using the GeoSAR mapping system, Geoscience and Remote Sensing Symposium, Vol. 1, 126 - 128